



Application of silver solid amalgam electrodes in electrochemical detection of DNA damage

Veronika Svitková¹ · Katarína Nemčeková¹ · Vlastimil Vyskočil²

Received: 30 November 2021 / Revised: 6 January 2022 / Accepted: 19 January 2022 / Published online: 7 February 2022
© Springer-Verlag GmbH Germany, part of Springer Nature 2022

Abstract

In this study, a mercury meniscus–modified silver solid amalgam electrode was used for the first time for the detection of UV-induced DNA damage. The integrity of the double-stranded DNA (dsDNA) layer was detected indirectly using the evaluation of the methylene blue reduction within its accumulation into dsDNA after the UV irradiation of the biosensor surface with two different wavelengths (254 nm and 365 nm), monitored by differential pulse voltammetry. Moreover, a simple electrochemical characterization of the biosensor surface was performed using cyclic voltammetry of the redox indicator hexaammineruthenium chloride (RuHex) present in the solution. Electrochemical impedance spectroscopy (EIS) was used in both cases for the verification of results. Individual electrochemical signals depend on the time of biosensor exposure to UV irradiation as well as on the selected wavelengths and are different for both used types of dsDNA (salmon sperm and calf thymus). The highest degradation degree up to 60% was observed using sensitive EIS of methylene blue after 10 min irradiation of the biosensor at 254 nm. The use of RuHex seems to be less sensitive for the detection of dsDNA structural changes, when the degradation degree up to 40% was observed, using EIS at the same conditions.

Keywords DNA damage · UV radiation · Amalgam electrode · Electrochemical biosensor · Methylene blue

Introduction

Electrochemical techniques in recent years raise increasing interest in detecting DNA damage mainly because of their simplicity, fast response, and low cost. A variety of different electrochemical strategies have been employed to detect DNA lesions, based on either the direct electrochemical response of guanine bases in DNA or the redox signal of electroactive probes that have specific interactions with DNA [1]. Ultraviolet (UV) radiation from the sun, especially

that characterized by shorter wavelengths and high frequencies, is associated with skin cancer and immunosuppression and caused damage to DNA due to the fact that DNA bases directly absorb UV photons [2]. This effect is determined by the formation of DNA lesions, which leads to the creation of covalent bonds between the pyrimidine bases and the formation of cyclobutane pyrimidine dimers [3]. Induction of DNA damage by solar UV irradiation can result in (i) misincorporation of bases during the replication process, (ii) hydrolytic damage, which results in deamination of bases, depurination, and depyrimidination, (iii) oxidative damage, caused by direct interaction of ionizing irradiations with the DNA molecules as well as mediated by UV irradiation-induced free radicals or reactive oxygen species (ROS), and (iv) formation of alkylating agents that may result in modified bases, all these depending on the type of UV irradiation [4].

In particular, the formation of ROS in living organisms is a well-known process, and their levels are regulated by enzymes or antioxidants. However, the excessive accumulation of ROS can possess a potential risk for human and animal health. The balance disturbance between ROS production and antioxidant activity is called oxidative stress, which

Published in the topical collection featuring *Promising Early-Career (Bio)Analytical Researchers* with guest editors Antje J. Baeumner, María C. Moreno-Bondi, Sabine Szunerits, and Qiuquan Wang.

✉ Veronika Svitková
veronika.svitkova@stuba.sk

¹ Institute of Analytical Chemistry, Faculty of Chemical and Food Technology, Slovak University of Technology in Bratislava, 81237 Bratislava, Slovakia

² UNESCO Laboratory of Environmental Electrochemistry, Department of Analytical Chemistry, Faculty of Science, Charles University, 12843 Prague, Czech Republic

is accompanied by the degradation of all cellular components (proteins, lipids, and DNA), leading to different types of diseases or genetic disorders. Regarding DNA damage as the result of an interaction between generated ROS radicals and a DNA molecule, various changes of the primary DNA structure can occur, ranging from the exchange/loss of DNA bases to the formation of strand breaks and cross-links [5].

For characterization of the DNA structure, indicators that bind to the DNA non-covalently (via intercalation of planar aromatic molecules between base pairs in the duplex DNA [6]) are of special interest [7, 8]. Methylene blue is an organic dye that belongs to the phenothiazine family, intercalates into dsDNA, and can be efficiently reduced through DNA-mediated charge transport [9, 10]. Several strategies have been employed to study the interaction between DNA and methylene blue [11, 12]. The detection of hybridization was accomplished by using the specific interaction of methylene blue with guanine [13]. Lin et al. [14] developed a dsDNA/graphene oxide-chitosan/AuNPs/GCE sensor for the detection of DNA damage induced by endocrine-disrupting compounds with the use of methylene blue as a redox indicator. García-González et al. [15] used methylene blue as an electroactive label covalently attached to ssDNA for the preparation of bioassay. Methylene blue was also used by De Grozals et al. [16] for DNA labeling.

Amalgam electrodes are environmentally friendly alternatives to mercury electrodes suitable for batch analysis or flow injection analysis. They are being considered as non-toxic alternative analytical tools to traditional mercury electrodes, with a broad negative potential window offering high hydrogen overpotential, good mechanical stability, and sufficient sensitivity in the determination of various electrochemically active organic compounds [17]. Several types of amalgam electrodes have been introduced in DNA analysis and DNA biosensor development, including detecting DNA hybridization [18] and DNA-chemical agent interactions [19]. Polished and mercury film-modified silver solid amalgam electrodes were used for the measurements of intrinsic redox and tensammetric voltammetric signals of single-stranded and double-stranded, linear, or supercoiled DNA, synthetic polynucleotides, and free adenine base [20] and for the voltammetric determination of adenine and guanine purine bases [21]. Mercury meniscus-modified silver solid amalgam electrodes (m-AgSAEs) were used by Danhel et al. [22, 23] for electrochemical studies of dsDNA modified by multi-redox labels. Only one publication from 2004 [24] was devoted to the detection of DNA damage caused by a cleaving agent at a silver solid amalgam electrode in connection with alternating current voltammetry. Here, the qualitative differences between the voltammetric behaviour of covalently closed supercoiled DNA and linear DNA allowed sensitive detection of strand breaks in DNA structure. Due to the difficulty of the whole procedure (when the copper cleaving complex

was prepared by mixing CuSO_4 and 1,10-phenanthroline), the researcher did not pay proper attention to the detection of DNA damage on amalgam electrodes.

Therefore, this study should provide a relatively fundamental attempt to move a bit further in this field, so the amalgam electrodes, on which the DNA is spontaneously immobilized very well, can compete with carbon electrodes, where the immobilization step is not always quite simple without previous modification.

In this study, methylene blue and hexaammineruthenium chloride (RuHex) as the redox-active molecules provide a highly sensitive way to detect UV-induced DNA damage at the m-AgSAE, which surface can be easily renewed, either mechanically (old meniscus is wiped off and after short polishing, a new one is formed) or electrochemically by a series of suitable potential cleaning pulses [25]. Two different types of dsDNA (salmon sperm and calf thymus) and two different wavelengths (254 nm and 365 nm) are used for the irradiation of the biosensor surface. A complex DNA biosensor response is based on difference pulse voltammetric (DPV) signal of the intercalative indicator methylene blue, cyclic voltammetric (CV) response of the RuHex redox indicator in solution, and modern electrochemical impedance spectroscopy (EIS) detection.

Materials and methods

Reagents

Low molecular salmon sperm dsDNA (ssp DNA) and calf thymus dsDNA (ct DNA) of final concentration 0.1 mg/mL obtained from Sigma-Aldrich, USA, were prepared by dilution with the 0.1 M phosphate buffer (PB) pH 7.0 and stored in the fridge at 4 °C. The stock solution of methylene blue (MB, $c = 1$ mM) was prepared by dissolving an accurately weighed amount of dye in deionised water and stored in the fridge at 4 °C. Working solutions of MB ($c = 0.01$ mM) were prepared freshly before every use. A 1 mM RuHex was used as a redox probe; a 0.1 M PB of pH 7.0 was prepared in the usual way and used as a supporting electrolyte; a 0.2 M potassium chloride solution (KCl) was used for the activation of the working electrode. Deionised water produced by a Milli-Q Plus system (Millipore, USA) was used to prepare all solutions. All reagents (Lach-Ner, Czech Republic) were of p.a. purity grade and stored in glass vessels at ambient temperature unless stated otherwise.

Apparatus

Voltammetric and impedimetric measurements were performed with the potentiostat Autolab III/FRA2 (Methrom Autolab, Switzerland) driven by a NOVA 1.11 software. All

measurements were carried out using a three-electrode system with a mercury meniscus–modified silver solid amalgam working electrode (m-AgSAE), silver/silver chloride reference electrode (Ag/AgCl/sat. KCl) and platinum auxiliary electrode, all contained in an electrochemical cell with a volume of 10 mL at ambient temperature. UV lamp (P-LAB, Czech Republic) with working wavelengths 254 nm (UV-C) and 365 nm (UV-A) and radiation power of 15 W (from 1 cm light source distance) was used for the UV irradiation. The pH measurements were carried out with a digital pH meter with a combined glass electrode.

Procedures

Before starting measurements, oxygen was removed from the measured solution by purging with nitrogen for 60 s. Before entering a voltammetric cell, nitrogen passed through a bubbler containing deionised water.

The m-AgSAE was prepared by immersing the surface of polished silver solid amalgam electrode (polished with alumina powder, 1.1 μm) into liquid mercury for 15 s while stirring and then rinsed with deionised water. After creating a new meniscus, each day before starting measurements and after electrode passivation, the working electrode was activated electrochemically in the 0.2 M KCl at -2200 mV for 300 s. Then, an electrochemical regeneration of the working electrode took place in order to reduce the influence of electrode passivation. Regeneration was based on 150 times switching the electrode potential between an initial ($E_{1\text{reg}}$) and a final ($E_{2\text{reg}}$) regeneration potential for 0.05 s.

The electrochemical DNA-based biosensor was prepared by dipping the m-AgSAE surface into 0.1 mg/mL ssp DNA or ct DNA solution in PB for 1 min under stirring. dsDNA was thus physically adsorbed on the surface of the activated m-AgSAE. The thus-prepared biosensor was washed with deionised water and then used. The surface of the DNA biosensor was exposed to UV irradiation with wavelength 254 nm or 365 nm for various periods of time from the 1 cm light source distance. After the exposure, the biosensor was rinsed with deionised water and the electrochemical measurements were performed.

DPV of MB was performed using the modulation amplitude of 50 mV, the modulation time of 100 ms, the interval time of 150 ms, the step potential of -3 mV, and the scan rate of 20 mV/s. The peak heights recorded using DPV were evaluated from the straight lines connecting the minima before and after the peak. The CV of RuHex was performed using the step potential of -3 mV and the scan rate of 20 mV/s. For the EIS of both, MB and RuHex, the polarization potential of -200 mV, the frequency range from 0.1 to 5000 Hz (51 frequency steps), and the amplitude of 10 mV were used. EIS data were obtained from Nyquist plots as an

imaginary impedance component against the real impedance component (at 5 k Ω) at each excitation frequency.

The DPV cathodic peak current of MB and the CV cathodic peak current of RuHex as well as the EIS imaginary impedance component against the real impedance component (of both MB and RuHex) are expressed as the relative values compared to the values obtained at the biosensors before application of the UV irradiation and are calculated using the ratio:

$$S_{rel} = \frac{S_1}{S_0} \times 100\% \quad (1)$$

where S_0 and S_1 are signals recorded before and after the UV-induced DNA damage at the biosensor.

All experiments were repeated three times ($n = 3$). The parameters of all mathematical and statistical quantities (for significant level $\alpha = 0.05$) were calculated using an Origin Pro 9.0 software (OriginLab, USA).

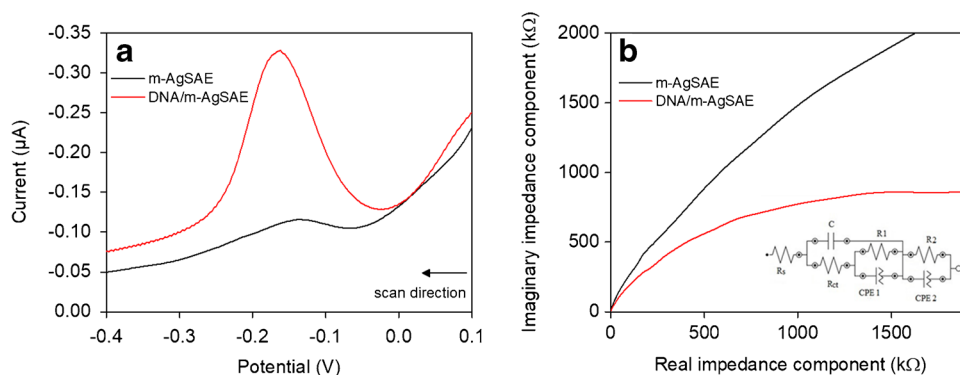
Results and discussion

Methylene blue and DNA interaction study

The electrochemical behaviour of DNA-MB interactions was investigated by means of DPV at the m-AgSAE. DP voltammogram of MB ($c = 0.01$ mM) (Fig. 1a) shows a cathodic reduction peak at around -0.15 V after 1 min of incubation at the bare m-AgSAE, while no significant adsorption of MB at the bare m-AgSAE was observed. However, with the concentration and incubation time increase, the adsorption of MB onto the surface of the m-AgSAE became more evident (not shown), which was undesirable for further measurements. At the sspDNA/m-AgSAE biosensor (Fig. 1a), the response of 0.01 mM MB solution was obtained after 1 min incubation which results in a slight shift of MB peak to lower potential values and a significant increase of this peak which can be described as the intercalation of the indicator into dsDNA [13]. The concentration and time of incubation of DNA had no significant effect. The concentration of dsDNA to form a layer (0.1 mg/mL), the time of the dsDNA spontaneous immobilization on the surface of the electrode (1 min), the concentration of MB (0.01 mM), and the time of the accumulation of MB into the dsDNA layer (1 min) were previously optimized for further biosensor development and applications [26]. The biosensor prepared as described above can be further used as a tool for DNA damage evaluation. The same trend was observed for ct DNA.

The behaviour of DNA-MB interaction was also investigated by means of EIS, where the charge transfer resistance of the sspDNA/m-AgSAE in the presence of MB in PB pH 7.0 was probed at -200 mV (Fig. 1b). In the Randles

Fig. 1 Electrochemical behaviour of MB at the m-AgSAE and the DNA/m-AgSAE biosensor: DP voltammograms (a) and Nyquist plots (b) of MB ($c_{\text{MB}} = 0.01 \text{ mM}$) measured at the m-AgSAE and at the sspDNA/m-AgSAE biosensor ($c_{\text{DNA}} = 0.1 \text{ mg/mL}$) after 1 min contact for the accumulation

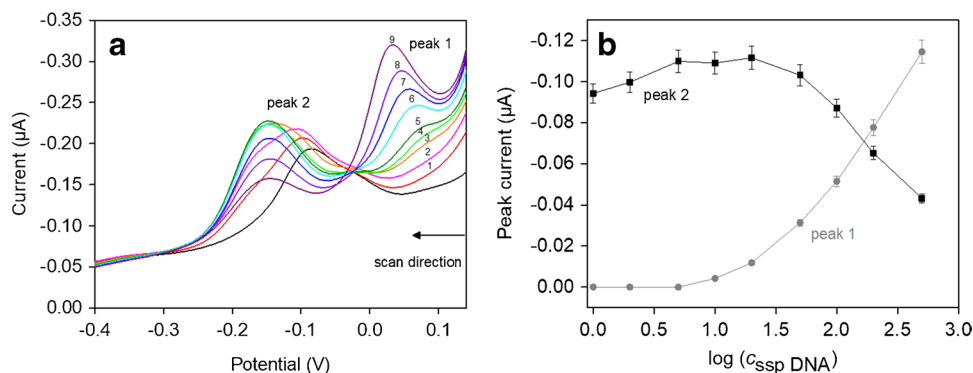


equivalent circuit model used for fitting the EIS spectra, R_s simulates the ohmic (contact) resistance; R_{ct} represents the charge transfer resistance of the electrode–electrolyte interface; the element C represents the capacitance of double electric layer which is charged simultaneously with the occurring electrochemical reaction. The experimental data are described by an equivalent electric circuit characteristic of the processes that include the adsorption of an intermediate compound; the double layer capacity and the adsorption capacity are replaced by the respective constant phase elements (CPE). This element contains many surface defects such as local charge inhomogeneities (from MB) or adsorbed species (from DNA). Consequently, in the Nyquist plot, the semicircle becomes flattened and exhibits the ideal profile of a purely diffusion-controlled reaction [27]. The impedance of this type of working electrode appeared almost as a linear line, which also indicated excellent conductivity, good electrocatalytic activity, and seamless electron transport on the electrode–electrolyte interface [28]. The resistance of the electron transfer is significantly lower at sspDNA/m-AgSAE compared to the unmodified electrode (Fig. 1b). This can be in correspondence with the fact that the positively charged MB is intercalated into the base pairs of negatively charged dsDNA while DNA film serves here as a bridge for enhanced charge transport which leads to increasing the conductivity and decreasing the resistance at the electrode surface [1]. Again, the same trend was observed for ct DNA experiments.

The voltammograms displayed in Fig. 2 illustrate the shift of the MB peak potential (around -0.1 V) toward more negative values, and also early increase and subsequent gradual decrease of the MB peak current values. Along with the increase of ssp DNA concentration, we can observe an increase of the new peak current values (around $+0.05 \text{ V}$) and a slight shift of the peak potential. The change of the electrochemical behaviour of both DNA and MB molecules can indicate a formation of a mutual complex. Such redox behaviour of MB in the presence of dsDNA is a well-defined mechanism that has an intercalative mode [29]. Similar behaviour was observed for ct DNA (not shown), when peak current increase and subsequent gradual decrease while accompanied with the slight shift of the peak potential values, however, this time, without the formation of a new peak.

These data showed that the observed electrochemistry is most efficient at DNA-modified electrodes when the redox probe is bound to the DNA attached at the electrode surface. The previous electrode surface passivation studies showed that in the case of intercalating MB, the DNA base pairs attached at the electrode surface provide a bridge for charge transport. As a consequence, surface passivation has no significant effect on the electrochemistry of MB [30]. Any electrochemical processes are possible to observe due to the fact that MB was employed as a reporter of DNA-mediated processes, as the surface is inaccessible to the molecule [9].

Fig. 2 Interaction study of MB and DNA at the m-AgSAE: DP voltammograms of MB ($c_{\text{MB}} = 0.01 \text{ mM}$) in the absence (black line) and presence of ssp DNA ($c_{\text{DNA}(1-9)} = 1, 2, 5, 10, 20, 50, 100, 200, \text{ and } 500 \text{ µg/L}$) (a) and the dependence of the I_{p1} (grey) and I_{p2} (black) on the $\log(c_{\text{DNA}})$ (b). Measured at the m-AgSAE after 1 min contact for the accumulation



Damage to DNA after UV irradiation of the biosensor in the presence of methylene blue

Two independent electrochemical techniques, i.e., DPV and EIS, were used to detect and evaluate changes in the DNA layer induced by UV irradiation (with wavelengths 254 nm and 365 nm) at the DNA/m-AgSAE biosensor surface using the redox response of MB. The detection strategies before and after the exposure of the biosensor to UV irradiation are schematically represented in Fig. 3. Firstly, the m-AgSAE surface was modified with dsDNA and the prepared biosensor was immersed into the solution of 0.01 mM MB. Upon intercalation of MB into the dsDNA structure, the cathodic peak of MB was registered (Fig. 3a). In order to detect the DNA damage, a newly prepared biosensor was exposed to daylight as well as to the UV irradiation of different wavelengths (254 and 365 nm) and then immersed in the MB solution (Fig. 3b). The formation of strand breaks and the release of dsDNA fragments from the electrode surface were detected indirectly via monitoring the decrease of the MB cathodic peak upon intercalation. In addition, these structural changes can be investigated using EIS which controls the charge transfer resistance before and after the breakage of the DNA chains. To detect the DNA damage by UV irradiation, exposure of the DNA biosensor to daylight was used as a control test. The relative change of MB cathodic peak current (Fig. 4a) and the relative change of the Nyquist plot values (Fig. 4b) indicated damage to ssp DNA as a progressive release of the degraded DNA fragments from the biosensor surface (decrease of the $I_{p,rel}$ and Z''_{rel} values). This degradation became deeper with the exposure time to UV

irradiation and was evidently the highest for the most harmful UV-C irradiation with a wavelength of 254 nm. Results showed the slight DNA degradation independent of the time of the irradiation for the wavelength 365 nm and also demonstrated the stability of the prepared biosensor at daylight.

On the other hand, the behaviour of ct DNA was somehow different. Although the deepest degradation of DNA was recorded again for UV-C irradiation of 254 nm, here the time dependence showed the opposite trend. The relative change of MB cathodic peak current (Fig. 4c) and the relative change of the Nyquist plot (Fig. 4d) were represented as an early decrease and subsequently gradual increase of the $I_{p,rel}$ and Z''_{rel} values. This can be probably due to the different structure of the DNA chain (10,000 base pairs, compared to ssp DNA with 200 base pairs), where the damage to DNA does not immediately represent the strand breaks and release of the DNA fragments from the electrode surface. In difference, the DNA layer exhibits damage by the opening of the helix structure and, therefore, to the intercalation with the MB present in the solution. For the wavelength 365 nm and for daylight were these values stable up to 10 min. The structure of ct DNA was found to be more stable under these conditions than the structure of ssp DNA; thus, ct DNA needs more time to be damaged because of its more difficult structure and length than ssp DNA.

Damage to DNA after UV irradiation of the biosensor in the presence of hexaammineruthenium chloride

Another approach how to detect damage to DNA at the m-AgSAE can be a use of a non-intercalating redox indicator

Fig. 3 Scheme for DNA damage detection at the dsDNA/m-AgSAE surface using MB: monitoring of MB redox response upon its intercalation to the dsDNA structure before (a) and after (b) the exposure to the irradiation using pulse voltammetric and impedimetric approaches

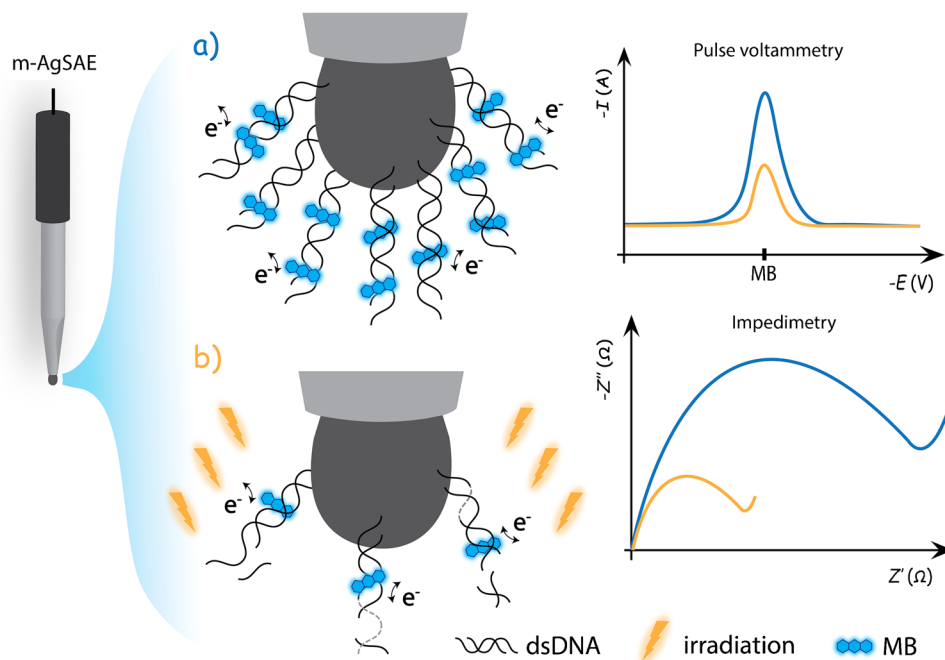
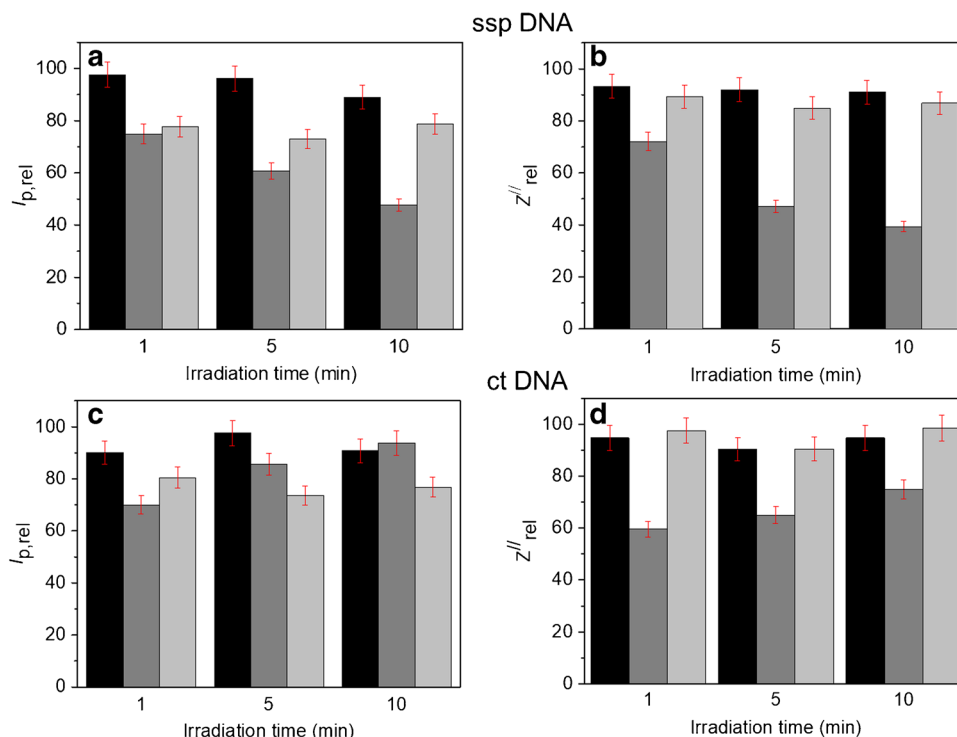


Fig. 4 Indirect electrochemical analysis of the DNA damage using response of 0.01 mM MB: the relative change of DPV cathodic peak current values $I_{p,rel}$ (left) and of the Nyquist plot values Z''_{rel} (right) at the sspDNA/m-AgSAE biosensor (**a, b**) and the ctDNA/m-AgSAE biosensor (**c, d**) after the exposure to UV irradiation (254 nm (dark grey) and 365 nm (light grey)) and to daylight (black) for a given time, evaluated using Eq. (1)

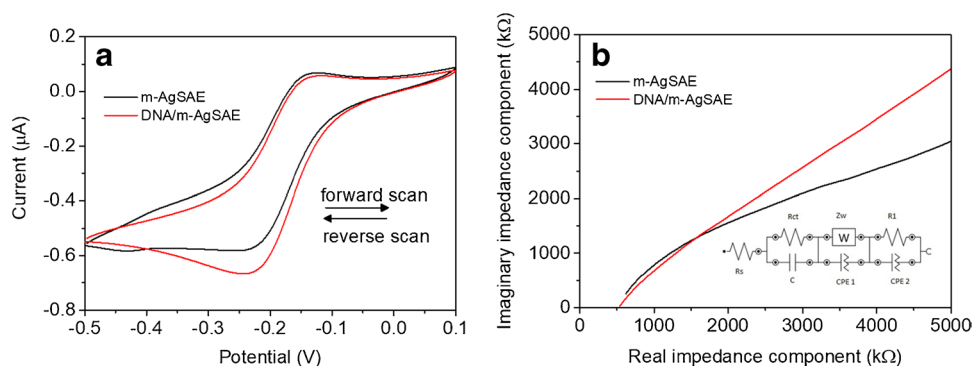


such as RuHex. It binds in the groove of DNA duplex, is reduced at approximately the same potential as MB, and associates with DNA through electrostatic and hydrogen-bonding interactions [30, 31]. Although RuHex is a well-known redox probe to determine the impedances and the electron transfer through self-assembled monolayers, its use in biosensor applications is still not fully developed for all types of electrode materials (it is mostly used for gold surfaces) [32].

Here, the CV and EIS of the m-AgSAE and the dsDNA/m-AgSAE biosensor took place in order to characterize the sensor before and after the modification step. CV curves of the probe manifested a pair of well-developed redox peaks. As Fig. 5a shows, the signal of the redox probe at CV measurements drifted to higher currents after the immobilization of dsDNA at the m-AgSAE surface. The EIS plot shown in

Fig. 5b consists of two regions. One is a semi-circular part in the high-frequency range and the other is a straight line in the low-frequency range. The semi-circular part corresponds to the charge transfer resistance (R_{ct}) between the electrode surface and the electrolyte solution. Also, its intercept at high frequencies on the real axis corresponds to the electrolyte resistance (R_s). The straight line corresponds to the diffusion-controlled process at low frequencies, representing the Warburg impedance (Z_w). After modification with the dsDNA layer, it almost became a straight line indicating an improvement in electron transfer because of increasing conductivity at the electrode surface. The enhanced charge transfer occurred since positively charged RuHex complexes are attracted by the immobilized negatively charged dsDNA [33]. The results obtained were in good agreement with CV measurements.

Fig. 5 Electrochemical behaviour of RuHex at the m-AgSAE and the DNA/m-AgSAE biosensor: CV (**a**) and Nyquist plots (**b**) of RuHex ($c_{RuHex} = 1$ mM) measured at the m-AgSAE and at the sspDNA/m-AgSAE biosensor ($c_{DNA} = 0.1$ mg/mL) after 1 min contact for the accumulation



Well, CV and EIS took place in order to evaluate UV-induced DNA damage after the irradiation of the biosensor surface for various periods of time from the 1 cm light source distance. Again, the DNA/m-AgSAE biosensor was exposed to UV irradiation of two different wavelengths (254 nm for UV-C and 365 nm for UV-A) and to daylight. A decrease of the CV cathodic peak current (Fig. 6a) in correspondence with a decrease in the Nyquist plot values (Fig. 6b) was the evidence of DNA damage under UV irradiation. The degradation of the biolayer became again deeper with the time of exposure to UV irradiation, which is most evident in the UV-C irradiation. The results again proved the stability of the biosensor response at daylight.

The same approach was applied to the biosensor with ct DNA attached to the electrode surface. Similarly, a decrease of the CV cathodic peak current was in correspondence with a decrease in the Nyquist plot values, but the sensitivity of the biosensor response was in all cases (for both wavelengths and daylight) comparable. The relative change of CV cathodic peak current values ($I_{p,rel}$) (Fig. 6c) and the relative change of the Nyquist plot values (Z''_{rel}) (Fig. 6d) obtained in these experiments are compared. This suggests that ssp DNA attached to the electrode surface, structurally not as complex as ct DNA, is more sensitive to the changes after the short-term UV irradiation.

In comparison with the use of intercalating MB, this concept was less sensitive for the detection of the structural changes of surface-attached DNA, which makes the introducing MB-based detection technique more convenient. It is

possible that in the case of RuHex, the DNA film serves to concentrate the molecule near the electrode surface; passivation of the surface could limit direct contact and, therefore, turns off the RuHex electrochemistry [30].

The approaches described in this study are, therefore, expected to provide quite substantial advances in the field of silver amalgam electrodes. Several strategies have been employed to study the detection of DNA damage caused by various physical and chemical agents [34–38], and many of them required chemically modified DNA sequences, e.g. thiol or amine modifications (which rapidly increases the cost), highly specialized equipment, and, in general, high adsorption times. Some of the works dealing with the evaluation of UV-induced DNA damage are summarized and compared in Table 1. In the case of silver amalgam electrodes, neither further modification of the electrode surface nor higher adsorption times are necessary, as the DNA probe is immobilized very well spontaneously compared to commonly used carbon-based or gold electrodes.

Conclusions

Electrochemical detection using a simple electrochemical DNA-based biosensor with mercury meniscus-modified silver solid amalgam working electrode is reported to evaluate UV-induced damage to a surface-attached double-stranded DNA. Three independent electrochemical techniques, (i) differential pulse voltammetric response

Fig. 6 Indirect electrochemical analysis of the DNA damage using response of 1 mM RuHex: the relative changes of CV cathodic peak current values $I_{p,rel}$ (left) and of the Nyquist plot values Z''_{rel} (right) at the sspDNA/m-AgSAE biosensor (**a**, **b**) and the ctDNA/m-AgSAE biosensor (**c**, **d**) after the exposure to UV irradiation (254 nm (dark grey) and 365 nm (light grey)) and to daylight (black) for a given time, evaluated using Eq. (1)

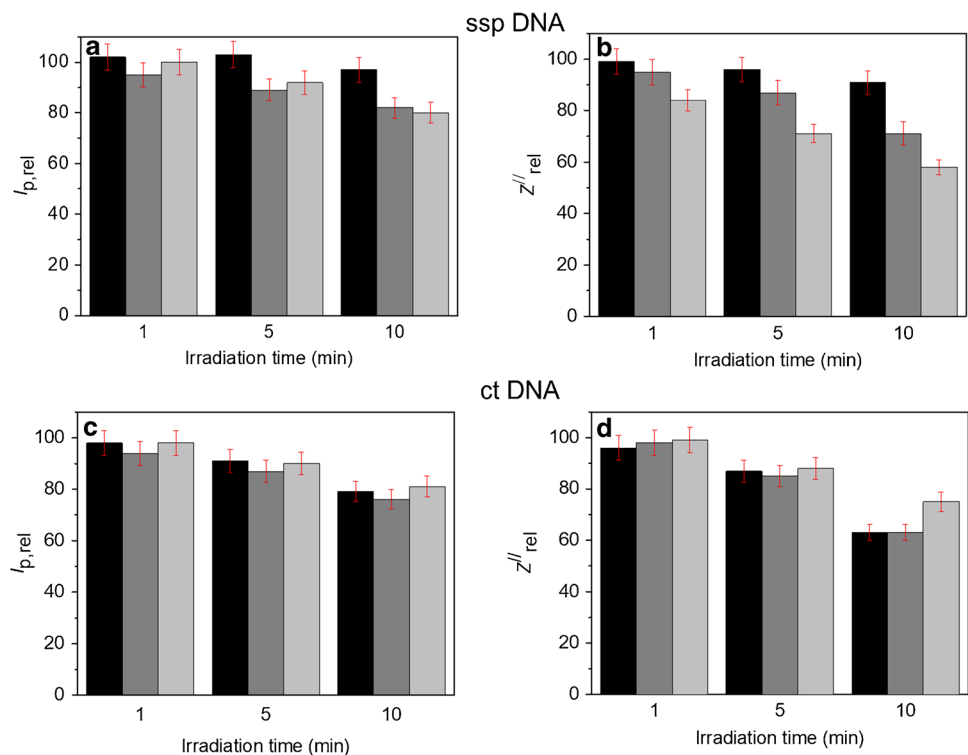


Table 1 Comparison of detection techniques, electrode materials and probes for the evaluation of UV-induced DNA damage using DNA-based biosensors

Electrode material	Indicator	Electrochemical technique	Irradiation time [min]	DNA damage degree [%]	Ref
SWCNTs-CHIT/SPCE	[Fe(CN) ₆] ^{3-/4-} , thioridazine	EIS	5	20	[8]
HOOC/SPCE	[Fe(CN) ₆] ^{3-/4-}	EIS	40	-	[39]
GCE	[Fe(CN) ₆] ^{3-/4-}	EIS	5	33	[40]
	PB	SWV		45	
GCE	[Fe(CN) ₆] ^{3-/4-}	CV	5	35	[41]
GCE	[Fe(CN) ₆] ^{3-/4-}	CV	5	43	[42]
	PB	SWV		69	
PDDA/MPA/AuE	[Co(phen) ₃] ³⁺	CV	75	-	[43]
	[Fe(CN) ₆] ^{3-/4-}	EIS			
PPy/GCE	NaCl	Amperometry	480	-	[44]
AuE	ferrocene	DPV	60	-	[45]
		EIS			
m-AgSAE	MB	DPV	5	55	this study
		EIS		60	
m-AgSAE	RuHex	CV	5	20	this study
		EIS		40	

Abbreviations: *AuE* gold electrode, *CHIT* chitosan, *CV* cyclic voltammetry, *GCE* glassy carbon electrode, *DPV* differential pulse voltammetry, *EIS* electrochemical impedance spectroscopy, *m-AgSAE* mercury meniscus-modified silver solid amalgam electrode, *MPA* 3-mercaptopropionic acid, *PDDA* polycationic poly(diallyldimethylammonium), *PPy* polypyrrole, *RuHex* hexaamineruthenium chloride, *SPCE* screen-printed carbon electrode, *SWCNTs* single-walled carbon nanotubes, *SWV* square-wave voltammetry

of DNA intercalator methylene blue, (ii) cyclic voltammetry of hexaammineruthenium chloride redox indicator, and (iii) electrochemical impedance spectroscopy in the presence of methylene blue or hexaammineruthenium chloride, were applied to characterize time changes of DNA structure when it is influenced by UV irradiation of different wavelengths. An amalgam working electrode, as an environmentally friendly alternative to traditional mercury electrodes, is reported here for the first time to detect damage to DNA. These approaches could provide a promising way for a simple and sensitive indication of DNA structural changes caused by various types of physical (drugs, pesticides, nanoparticles) and chemical agents (UV light) from the environment. For example, UV-C is a well-characterized genotoxic agent that is used to study DNA damage and repair [46]. Recently, it has become relevant in various medical applications, including acting as an anticancer agent [47] and as a disinfectant for localized treatments of multidrug-resistant infections [48, 49]. On the other hand, the monitoring of DNA damage represents an important aspect of cancer treatment. However, until recently, the available methods were limited by poor sensitivity and/or long turn-around time. Thus, the emergence of a rapid, sensitive method to quantify the DNA damage that is apparent shortly after treatment has great potential to monitor not only the response of the tumour but also the effects of the treatment on “at-risk” normal tissues, to thus assess the therapeutic ratio of used chemotherapeutics.

Acknowledgements Technical, material, and intellectual support from the Metrohm Czech Republic is gratefully acknowledged.

Funding This work was supported by the Scientific Grant Agency VEGA of the Slovak Republic (Project No. 1/0489/16). VV, moreover, received from the Czech Science Foundation (Project GACR No. 20-01417 J) financial support for this research. VS received from the Erasmus + Program of the Slovak Republic support for her research stay at the Charles University in Prague.

The authors alone are responsible for the content and writing of the paper. The publication has been approved by all co-authors.

Declarations

Conflict of interest The authors declare no conflict of interest.

References

1. Paleček E, Bartošík M. Electrochemistry of nucleic acids. *Chem Rev.* 2012;112:3427–81. <https://doi.org/10.1021/cr200303p>.
2. Santonicola MG, Coscia MG, Sirilli M, Laurenzi S. Nanomaterial-based biosensors for a real-time detection of biological damage by UV light. *Proc Annual Int Conf IEEE Eng Med Biol Soc (EMBC).* 2015;4391–94.
3. Ravanat J-L, Douki T, Cadet J. Direct and indirect effects of UV radiation on DNA and its components. *J Photochem Photobiol B, Biol.* 2001;63:88–102. [https://doi.org/10.1016/S1011-1344\(01\)00206-8](https://doi.org/10.1016/S1011-1344(01)00206-8).
4. Rastogi RP, Richa, Kumar A, Tyagi MB, Sinha RP. Molecular mechanisms of ultraviolet radiation-induced DNA damage and

- repair. *J Nucleic Acids*. 2010;2010:592980. <https://doi.org/10.4061/2010/592980>.
- Hájková A, Barek J, Vyskočil V. Electrochemical DNA biosensor for detection of DNA damage induced by hydroxyl radicals. *Bioelectrochem*. 2017;116:1–9. <https://doi.org/10.1016/j.bioelechem.2017.02.003>.
 - Fojta M, Daňhel A, Havran L, Vyskočil V. Recent progress in electrochemical sensors and assays for DNA damage and repair. *TrAC - Trends Anal Chem*. 2016;79:160–7. <https://doi.org/10.1016/j.trac.2015.11.018>.
 - Gebala M, Stoica L, Neugebauer S, Schuhmann W. Label-free detection of DNA hybridization in presence of intercalators using electrochemical impedance spectroscopy. *Electroanalysis*. 2009;21:325–31. <https://doi.org/10.1002/elan.200804388>.
 - Hlavata L, Benikova K, Vyskocil V, Labuda J. Evaluation of damage to DNA induced by UV-C radiation and chemical agents using electrochemical biosensor based on low molecular weight DNA and screen-printed carbon electrode. *Electrochim Acta*. 2012;71:134–9. <https://doi.org/10.1016/j.electacta.2012.03.119>.
 - Gorodetsky AA, Buzzeo MC, Barton JK. DNA-mediated electrochemistry. *Bioconjug Chem*. 2009;19:2285–96. <https://doi.org/10.1021/bc8003149>.
 - Zhang Y, Hu N. Cyclic voltammetric detection of chemical DNA damage induced by styrene oxide in natural dsDNA layer-by-layer films using methylene blue as electroactive probe. *Electrochem Commun*. 2007;9:35–41. <https://doi.org/10.1016/j.elecom.2006.08.032>.
 - Arias P, Ferreyra NF, Rivas GA, Bollo S. Glassy carbon electrodes modified with CNT dispersed in chitosan: analytical applications for sensing DNA-methylene blue interaction. *J Electroanal Chem*. 2009;634:123–6. <https://doi.org/10.1016/j.jelechem.2009.07.022>.
 - Yau HCM, Chan HL, Yang M. Electrochemical properties of DNA-intercalating doxorubicin and methylene blue on n-hexadecyl mercaptan-doped 5-thiol-labeled DNA-modified gold electrodes. *Biosens Bioelectron*. 2003;18:873–9. [https://doi.org/10.1016/S0956-5663\(02\)00161-6](https://doi.org/10.1016/S0956-5663(02)00161-6).
 - Kara P, Kerman K, Ozkan D, Meric B, Erdem A, Ozkan Z, Ozsoz M. Electrochemical genosensor for the detection of interaction between methylene blue and DNA. *Electrochem Commun*. 2002;4:705–9. [https://doi.org/10.1016/S1388-2481\(02\)00428-9](https://doi.org/10.1016/S1388-2481(02)00428-9).
 - Lin X, Ni Y, Kokot S. An electrochemical DNA-sensor developed with the use of methylene blue as a redox indicator for the detection of DNA damage induced by endocrine-disrupting compounds. *Anal Chim Acta*. 2015;867:29–37. <https://doi.org/10.1016/j.aca.2015.02.050>.
 - García-González R, Costa-García A, Fernández-Abedul MT. Methylene blue covalently attached to single stranded DNA as electroactive label for potential bioassays. *Sensors Actuators B Chem*. 2014;191:784–90. <https://doi.org/10.1016/j.snb.2013.10.037>.
 - De Crozals G, Farre C, Sigaud M, Fortgang P, Sanglar C, Chaix C. Methylene blue phosphoramidite for DNA labelling. *Chem Commun*. 2015;51:4458–61. <https://doi.org/10.1039/C4CC10164B>.
 - Yosypchuk B, Fojta M, Barek J. Amalgam electrodes as tool for study of environmental important compounds and for detection of DNA damages. *Int Conf Dev Energy, Environ Econ – Proc*. 2010;146–150.
 - Yosypchuk B, Fojta M, Havran L, Heyrovský M, Paleček E. Voltammetric behavior of osmium-labeled DNA at mercury meniscus-modified solid amalgam electrodes. Detecting DNA hybridization. *Electroanalysis*. 2006;18:186–94. <https://doi.org/10.1002/elan.200503392>.
 - Krejčova Z, Barek J, Vyskocil V. Voltammetric determination of fenitrothion and study of its interaction with DNA at a mercury meniscus modified silver solid amalgam electrode. *Monatshfte fur Chemie*. 2016;147:135–42. <https://doi.org/10.1007/s00706-015-1595-4>.
 - Fadrná R, Cahová-Kucharíková K, Havran L, Yosypchuk B, Fojta M. Use of polished and mercury film-modified silver solid amalgam electrodes in electrochemical analysis of DNA. *Electroanalysis*. 2005;17:452–9. <https://doi.org/10.1002/elan.200403181>.
 - Fadrná R, Yosypchuk B, Fojta M, Navrátil T, Novotný L. Voltammetric determination of adenine, guanine, and DNA using liquid mercury free polished silver solid amalgam electrode. *Anal Lett*. 2004;37:399–413. <https://doi.org/10.1081/Al-120028615>.
 - Danhel A, Raindlova V, Havran L, Pivonkova H, Hocek M, Fojta M. Electrochemical behaviour of 2,4-dinitrophenylhydrazine as multi-redox centre DNA label at mercury meniscus modified silver solid amalgam electrode. *Electrochim Acta*. 2014;126:122–31. <https://doi.org/10.1016/j.electacta.2013.09.147>.
 - Danhel A, Raindlova V, Havran L, Barek J, Hocek M, Fojta M. Voltammetric study of dsDNA modified by multi-redox label based on N-methyl-4-hydrazino-7-nitrobenzofurazan. *Electrochim Acta*. 2014;129:348–57. <https://doi.org/10.1016/j.electacta.2014.02.137>.
 - Kucharíková K, Novotný L, Yosypchuk B, Fojta M. Detecting DNA damage with a silver solid amalgam electrode. *Electroanalysis*. 2004;16:410–4. <https://doi.org/10.1002/elan.200302874>.
 - Barek J, Fischer J, Moreira JC, Wang J. Voltammetric and amperometric determination of biologically active organic compounds using various types of silver amalgam electrodes. In: Kalcher K, Metelka R, Svancara K, Vytras K, editors. *Sensing in Electroanalysis*, Vol 8. University Press Centre, Pardubice, Czech Republic; 2014. pp. 35–47.
 - Svitková V, Vyskočil V. Electrochemical behaviour of methylene blue at bare and DNA-modified silver solid amalgam electrodes. *J Solid State Electrochem*. 2022; after revisions.
 - Cesiulis H, Tsyntaru N, Ramnavicius A, Ragoisha G. The study of thin films by electrochemical impedance spectroscopy. In: Tiginyanu I, Topala P, Ursaki V, editors. *Nanostructured and Thin Films for Multifunctional Applications*. Springer: Switzerland; 2016. p. 3–42.
 - Al-Qasbi N, Hameed A, Khan AN, Aslam M, Ismail IMI, Soomro MT. Mercury meniscus on solid silver amalgam electrode as a sensitive electrochemical sensor for tetrachlorvinphos. *J Saudi Chem Soc*. 2018;22:496–507. <https://doi.org/10.1016/j.jscs.2016.07.005>.
 - Li WY, Xu JG, He XW. Characterization of the binding of methylene blue to DNA by spectroscopic methods. *Anal Lett*. 2000;33:2453–64. <https://doi.org/10.1080/00032710008543201>.
 - Boon EM, Jackson NM, Wightman MD, Kelley SO, Hill MG, Barton JK. Intercalative stacking: a critical feature of DNA charge-transport electrochemistry. *J Phys Chem B*. 2003;107:11805–12. <https://doi.org/10.1021/jp030753i>.
 - Dai S, Lu W, Wang Y, Yao B. Universal DNA biosensing based on instantaneously electrostatic attraction between hexaammineruthenium (III) and DNA molecules. *Biosens Bioelectron*. 2019;127:101–7. <https://doi.org/10.1016/j.bios.2018.12.019>.
 - Schrattenecker JD, Heer R, Melnik E, Maier T, Faflek G, Hainberger R. Hexaammineruthenium (II)/(III) as alternative redox-probe to hexacyanoferrat (II)/(III) for stable impedimetric biosensing with gold electrodes. *Biosens Bioelectron*. 2019;127:25–30. <https://doi.org/10.1016/j.bios.2018.12.007>.
 - Rafique S, Khan S, Bashir S, Nasir R. Facile development of highly sensitive femtomolar electrochemical DNA biosensor using gold nanoneedle-modified electrode. *Chem Papers*. 2020;74:229–38. <https://doi.org/10.1007/s11696-019-00874-y>.
 - Liang M, Guo L. Photoelectrochemical DNA sensor for the rapid detection of DNA damage induced by styrene oxide and the Fenton reaction. *Environ Sci Technol*. 2007;41:658–64. <https://doi.org/10.1021/es0617688>.

35. Liu Y, Jia S, Guo LH. Development of microplate-based photo-electrochemical DNA biosensor array for high throughput detection of DNA damage. *Sensors Actuators B Chem.* 2012;161:334–40. <https://doi.org/10.1016/j.snb.2011.10.041>.
36. Ziyatdinova G, Labuda J. Complex electrochemical and impedimetric evaluation of DNA damage by using DNA biosensor based on a carbon screen-printed electrode. *Anal Methods.* 2011;3:2777–82. <https://doi.org/10.1039/c1ay05403a>.
37. Oliveira SCB, Oliveira-Brett AM. In situ DNA oxidative damage by electrochemically generated hydroxyl free radicals on a boron-doped diamond electrode. *Langmuir.* 2012;28:4896–901.
38. Zitka O, Krizkova S, Skalickova S, Kopel P, Babula P, Adam V, Kizek R (2013) Electrochemical study of DNA damaged by oxidation stress. *Comb Chem High Throughput Screen.* 2013;16:130–41. <https://doi.org/10.2174/1386207311316020007>.
39. Mousavisani SZ, Raoof JB, Cheung KY, Camargo ARH, Ruzgas T, Turner APF, Mak WC. Integrating an ex-vivo skin biointerface with electrochemical DNA biosensor for direct measurement of the protective effect of UV blocking agents. *Biosens Bioelectron.* 2019;128:159–65. <https://doi.org/10.1016/j.bios.2018.12.025>.
40. Svitkova V, Blaskovicova J, Tekelova M, Kallai BM, Ignat T, Horackova V, Skladal P, Kopel P, Adam V, Farkasova D, Labuda J. Assessment of CdS quantum dots effect on UV damage to DNA using a DNA/quantum dots structured electrochemical biosensor and DNA biosensing in solution. *Sensors Actuators B Chem.* 2017;243:435–44. <https://doi.org/10.1016/j.snb.2016.11.160>.
41. Blaškovičová J, Sochr J, Koutsogiannis A, Diamantidou D, Kopel P, Adam V, Labuda J. Detection of ROS generated by UV-C irradiation of CdS quantum dots and their effect on damage to chromosomal and plasmid DNA. *Electroanalysis.* 2018;30:698–704. <https://doi.org/10.1002/ELAN.201700648>.
42. Hlavata L, Striesova I, Ignat T, Blaskovisova J, Ruttkay-Nedecky B, Kopel P, Adam V, Kizek R, Labuda J. An electrochemical DNA-based biosensor to study the effects of CdTe quantum dots on UV-induced damage of DNA. *Microchim Acta.* 2015;182:1715–22. <https://doi.org/10.1007/s00604-015-1502-z>.
43. Yin CX, Yang T, Zhang W, Zhou XD, Jiao K. Electrochemical biosensing for dsDNA damage induced by PbSe quantum dots under UV irradiation. *Chinese Chem Lett.* 2010;21:716–9. <https://doi.org/10.1016/j.ccllet.2009.12.025>.
44. Wang J, Jiang M, Kawde AN. Flow detection of UV radiation-induced DNA damage at a polypyrrole-modified electrode. *Electroanalysis.* 2001;13:537–40.
45. Wei W, Ni Q, Pu Y, Yin L, Liu S. Electrochemical biosensor for DNA damage detection based on exonuclease III digestions. *J Electroanal Chem.* 2014;714–715:25–9. <https://doi.org/10.1016/j.jelechem.2013.12.018>.
46. Fendyr A, Varma S, Lo CT, Voldman J. Cell-based biosensor to report DNA damage in micro- and nanosystems. *Anal Chem.* 2014;86:7598–605. <https://doi.org/10.1021/ac501412c>.
47. Pujari I, Thomas A, Thomas J, Jhavar N, Guruprasad KP, Rai PS, Satyamoorthy K, Babu VS. Cytotoxicity and radiosensitizing potency of Moscatilin in cancer cells at low radiation doses of X-ray and UV-C. *3 Biotech.* 2021;11:281. <https://doi.org/10.1007/s13205-021-02827-3>.
48. Casini B, Tuvo B, Cristina ML, Spagnolo AM, Totaro M, Bagiani A, Privitera GP. Evaluation of an ultraviolet C (UVC) light-emitting device for disinfection of high touch surfaces in hospital critical areas. *Int J Environ Res Public Health.* 2019;16:3572. <https://doi.org/10.3390/IJERPH16193572>.
49. Rock C, Hsu Y-J, Curless MS, Carroll KC, Ross Howard T, Carson KA, Cummings S, Anderson M, Milstone AM, Maragakis LL. Ultraviolet-C light evaluation as adjunct disinfection to remove multidrug-resistant organisms. *Clin Infect Dis.* 2021. <https://doi.org/10.1093/CID/CIAB896>.

Publisher's note Springer Nature remains neutral with regard to jurisdictional claims in published maps and institutional affiliations.